ARTHRITIS & RHEUMATOLOGY
Vol. 68, No. 4, April 2016, pp 1013–1025
DOI 10.1002/art.39477

Antifibrotic, Antioxidant, and Immunomodulatory Effects of Mesenchymal Stem Cells in HOCl-Induced Systemic Sclerosis

Alexandre T. J. Maria,[1] Karine Toupet,[1] Claire Bony,[1] Nelly Pirot,[2] Marie-Catherine Vozenin,[3] Benoît Petit,[3] Pascal Roger,[4] Frédéric Batteux,[5] Alain Le Quellec,[6] Christian Jorgensen,[7] Danièle Noël,[1] and Philippe Guilpain[1]

Objective. **Systemic sclerosis (SSc) is a rare intractable disease with unmet medical need and fibrosis-related mortality. Absence of efficient treatments has prompted the development of novel therapeutic strategies, among which mesenchymal stem cells/stromal cells (MSCs) or progenitor stromal cells appear to be one of the most attractive options. The purpose of this study was to use the murine model of hypochlorite-induced SSc to investigate the systemic effects of MSCs on the main features of the diffuse form of the disease: skin and lung fibrosis, autoimmunity, and oxidative status.**

Methods. **We compared the effects of different doses of MSCs (2.5×10^5, 5×10^5, and 10^6) infused at different time points. Skin thickness was assessed during the experiment. At the time of euthanasia, biologic parameters were quantified in blood and tissues (by enzyme-linked immunosorbent assay, quantitative reverse transcription–polymerase chain reaction, assessment of collagen content). Assessments of histology and immunostaining were also performed.**

Results. **A lower expression of markers of fibrosis (*Col1*, *Col3*, *Tgfb1*, and *aSma*) was observed in both skin and lung following MSC infusion, which was consistent with histologic improvement and was inversely proportional to the injected dose. Importantly, sera from treated mice exhibited lower levels of anti–Scl-70 autoantibodies and enhanced antioxidant capacity, confirming the systemic effect of MSCs. Of interest, MSC administration was efficient in both the preventive and the curative approach. We further provide evidence that MSCs exerted an antifibrotic role by normalizing extracellular matrix remodeling parameters as well as reducing proinflammatory cytokine levels and increasing antioxidant defenses.**

Conclusion. **The results of this study demonstrate the beneficial and systemic effects of MSC administration in the HOCl murine model of diffuse SSc, which is a promising finding from a clinical perspective.**

Systemic sclerosis (SSc) is a rare and severe connective tissue disorder characterized by multivisceral fibrosis due to excessive collagen deposition, vasculopathy, and autoimmunity. Skin sclerosis and Raynaud's phenomenon are the main clinical features, which exhibit a strong effect on quality of life, whereas involvement of multiple organs, such as pulmonary fibrosis, is life-threatening and intractable. The conventional therapeutic approach is based on symptomatic treatment or immunosuppression, but it is ineffective in curing the most severe involvement, thus leading to the need for palliative care (oxygen therapy, cardiopulmonary trans-

Supported by the INSERM Institute, the University of Montpellier I, Montpellier-Nîmes University Hospital, the Association des Sclérodermiques de France, and the national infrastructure ECELLFRANCE: Development of a National Adult Mesenchymal Stem Cell–Based Therapy Platform, which is supported by the Agence Nationale pour la Recherche (ANR-11-INSB-005). Dr. Maria's work was supported by a fellowship from the French Health Ministry and the INSERM Institute.

[1]Alexandre T. J. Maria, MD, Karine Toupet, PhD, Claire Bony, MS, Danièle Noël, PhD, Philippe Guilpain, MD, PhD: INSERM U1183, St. Eloi Hospital, and Montpellier University Medical School, Montpellier, France; [2]Nelly Pirot, PhD: INSERM U1194 and UMS BioCampus Montpellier, Montpellier, France; [3]Marie-Catherine Vozenin, PhD, Benoît Petit, BTEC: University Hospital of Lausanne (CHUV), Lausanne, Switzerland; [4]Pascal Roger, MD, PhD: Montpellier University Medical School, Montpellier, France, and Caremeau Hospital, Nîmes, France; [5]Frédéric Batteux, MD, PhD: Paris Descartes University and EA1833, Paris, France; [6]Alain Le Quellec, MD, PhD: St. Eloi Hospital and Montpellier University Medical School, Montpellier, France; [7]Christian Jorgensen, MD, PhD: INSERM U1183, St. Eloi Hospital, Montpellier University Medical School, and Lapeyronie Hospital, Montpellier, France.

Drs. Noël and Guilpain contributed equally to this work.

Dr. Le Quellec has received speaking fees from Actelion (less than $10,000).

Address correspondence to Danièle Noël, PhD, INSERM U1183, Institute for Regenerative Medicine and Biotherapy, St. Eloi Hospital, 80 Avenue Augustin Fliche, 34295 Montpellier Cedex 5, France. E-mail: daniele.noel@inserm.fr.

Submitted for publication January 5, 2015; accepted in revised form October 13, 2015.

plantation) (1). During the last decade, hematopoietic stem cell transplantation has been proposed in SSc, but this approach is restricted by several limitations, such as high levels of toxicity and treatment-related mortality, requiring precise selection of patients (2). Consequently, SSc remains an incurable disease with severe fibrosis-related morbidity and mortality, in which novel and potent therapeutic approaches are being sought.

Recently, the usefulness of multipotent mesenchymal stem cells/stromal cells (MSCs) or progenitor stromal cells for the treatment of autoimmune diseases, including SSc, has been explored, and MSCs are currently under evaluation in clinics (3). MSCs are adult multipotent progenitor cells that are present in connective tissues such as bone marrow, adipose tissue, synovium, placenta, and umbilical cord. They are characterized by plastic adherence in culture, with a fibroblast-like morphology, a combination of positive surface markers (such as CD73, CD90, CD105), and an ability to differentiate into several lineages (osteoblasts, chondrocytes, and adipocytes). MSCs also display immunomodulatory properties, as shown in preclinical and clinical studies in rheumatoid arthritis, graft-versus-host disease, multiple sclerosis, systemic lupus erythematosus, and Crohn's disease (4–8). In refractory SSc, analysis of 6 clinical cases suggested that systemic infusion of MSCs may provide a therapeutic benefit (9,10). Nevertheless, the complex and specific features of SSc compared with other autoimmune diseases raise numerous questions that are still to be solved in preclinical studies.

Most studies performed to date have focused on the antifibrotic properties of MSCs in lung or skin and in the murine bleomycin-induced model of fibrosis, which does not encompass the systemic nature of SSc (11,12). In contrast, the HOCl-induced model of SSc is based on the repeated exposure of mice to oxidative stress, and after 6 weeks, HOCl-injected mice show collagen deposition in skin and lungs, some vascular abnormalities, advanced oxidation protein products (AOPPs) in serum, and anti–Scl-70 autoantibody production (13). The unique feature of this model lies in the ability to investigate the systemic effects of treatment in diffuse SSc, where lung and skin fibrosis coexist. We describe herein our findings of the therapeutic effects of MSCs in the HOCl-induced model of SSc: modulation of inflammation, oxidative balance, and tissue remodeling.

MATERIALS AND METHODS

Experimental design and animals. SSc was induced by daily intradermal injections of HOCl, as previously described (13). Control mice received daily injections of phosphate buffered saline (PBS). The studies were performed according to the Laboratory Animal Care guidelines with approval from the Regional Ethics Committee on Animal Experimentation (CEEA-LR-11054). All experiments were performed in BALB/c mice, except for the biodistribution study, which was performed in C57BL/6 mice. HOCl-injected mice received an infusion of 2.5×10^5, 5×10^5, or 10^6 MSCs in the tail vein at the time points indicated below. Skin, lung, and blood samples for molecular and histologic analyses were obtained at the time of euthanasia.

Isolation and culture of MSCs. MSCs from BALB/c or C57BL/6 green fluorescent protein (GFP)–positive mice were isolated from bone marrow, cultured, and characterized as described elsewhere (14). Cells were used before passage 15.

Histopathologic analysis. Sections (5 μm thick) of paraffin-embedded samples were stained with Masson's trichrome or immunostained with antibodies to α-smooth muscle actin (α-SMA) (1:100 dilution, catalog no. ab5694; Abcam), transforming growth factor β (TGFβ) (1:100 dilution, catalog no. ab66043; Abcam), Ki-67 (SP6) (1:200 dilution, catalog no. VP-RM04; Vector), CD3ϵ (M-20) (1:250 dilution, catalog no. sc-1127; Santa Cruz Biotechnology), F4/80 (1:50 dilution, catalog no. MF4800; Invitrogen), or paired box protein 5 (PAX-5) (1:250 dilution, sc-1974 [C-20]; Santa Cruz Biotechnology). Slides for histologic assessment were scanned using a NanoZoomer (Hamamatsu) or Pannoramic 250 Flash II (3DHistech) slide scanner for immunofluorescence. Mean dermal thickness was calculated at more than 30 points in each section using ImageJ software (National Institutes of Health). The extent of immunostaining was quantified using Definiens Tissue Studio software.

Quantitative reverse transcription–polymerase chain reaction (qRT-PCR) analysis. RNA was extracted from crushed samples using an RNeasy Mini kit (Qiagen). RNA (1 μg) was then reverse transcribed using Moloney murine leukemia virus reverse transcriptase (Invitrogen). Quantitative PCR was performed on 20 ng of complementary DNA using LightCycler 480 SYBR Green I Master and a real-time PCR instrument (Roche Applied Science). Primers were designed using the web-based applications Primer3 and BLAST (available upon request from the corresponding author). Samples were normalized to the expression of messenger RNA (mRNA) for the TATA box binding protein (TBP) gene for tissue samples or GAPDH for MSC cultures. The results were reported relative to the expression of these housekeeping genes using the formula $2^{-\Delta C_t}$ or as the fold increase in expression using the formula $2^{-\Delta\Delta C_t}$.

Analysis of GFP expression by qPCR. DNA was extracted using a DNeasy blood and tissue kit (Qiagen). Quantitative PCR was performed with 80 ng of DNA on a real-time PCR instrument (Viia7; Applied Biosystems) using SYBR Green Master mix and GFP primers (available upon request from the corresponding author). Results were compared with a standard curve of serial dilutions of GFP+ cells and then extrapolated to the whole organ for quantification, as previously described (15).

Tissue collagen content and lung phosphorylated Smad3 content. Collagen content in tissues was assayed according to the quantitative dye-binding Sircol method, using acid–pepsin extraction (Biocolor). The results were expressed as the collagen content in skin (μg/mm^2) and lung (μg/mg). Phosphorylated Smad3 was measured in lungs using an InstantOne enzyme-linked immunosorbent assay (ELISA) (eBio-

science). The results were expressed as arbitrary units per milligram of lung.

Determination of serum AOPP levels, total antioxidant capacity, and anti–Scl-70 levels. AOPP concentrations were measured by spectrophotometry as previously described (16). The results were expressed as chloramine T equivalents (μM). The total antioxidant capacity in a 1:10 dilution of serum was determined using an antioxidant assay kit (Cayman). The results were expressed as Trolox equivalents (mM). Anti–Scl-70 antibodies were detected in sera (1:5 dilution) using an Scl-70 Ig ELISA kit (Abnova).

Statistical analysis. All quantitative data were expressed as the mean ± SEM. Data were compared using the Mann-Whitney test for nonparametric values, Student's *t*-test for parametric values, and one-way ANOVA for more than 2 groups. For correlations, regression analysis was performed with Pearson's rank correlation test. All statistical analyses were performed using GraphPad Prism 6 software for Mac OS. *P* values less than 0.05 were considered significant.

RESULTS

Induction of skin and lung fibrosis and production of anti–topoisomerase I antibodies following HOCl injection. The HOCl model of SSc has been previously described (13), but the timing and the molecular characterization of the fibrotic process have not been investigated so far. We therefore recovered tissue samples at different time points and quantified several markers of fibrosis by qRT-PCR. Compared with PBS-injected

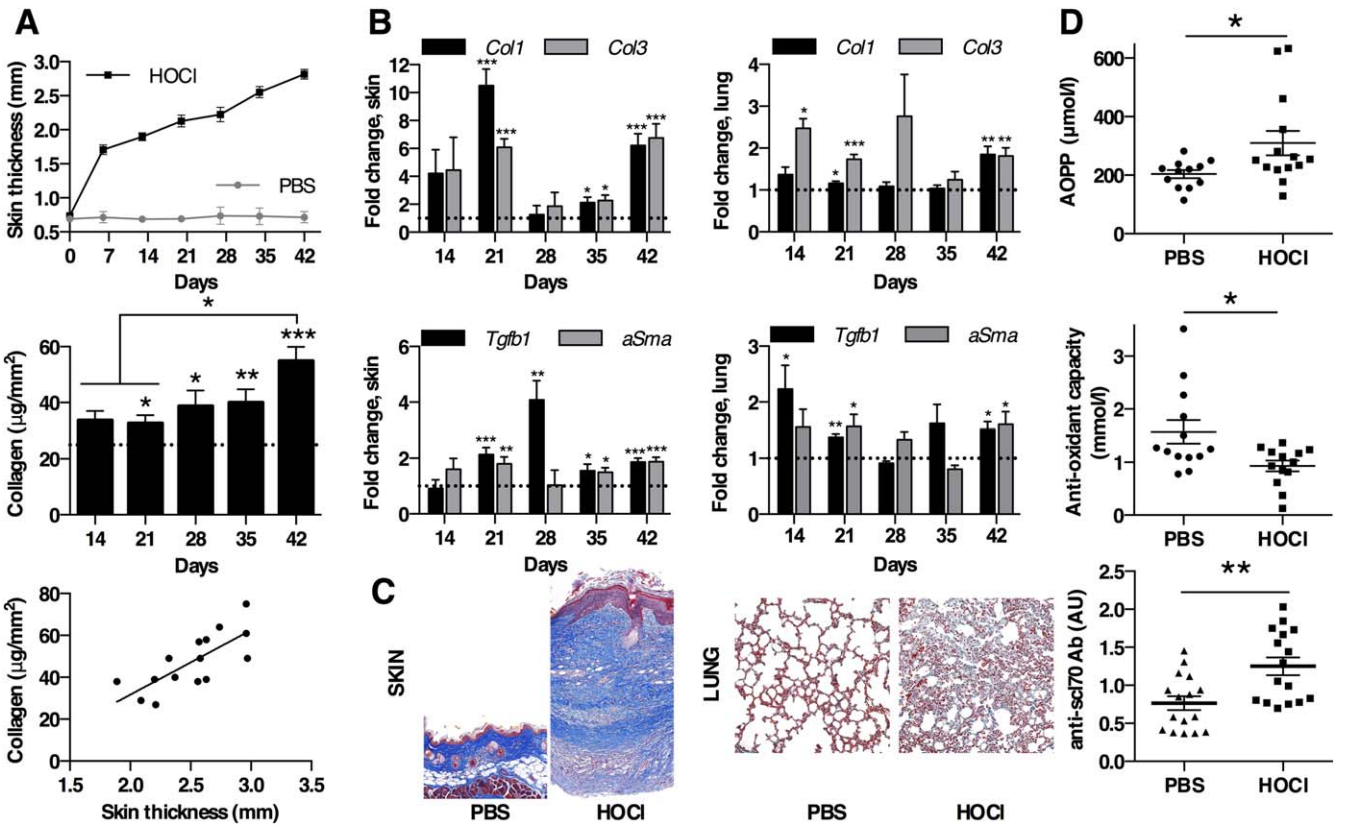

Figure 1. HOCl induction of skin and lung fibrosis and anti–topoisomerase I antibody (Ab) production. **A,** Skin thickness in HOCl-injected and phosphate buffered saline (PBS)–injected mice (top). Between-group comparisons at each time point from day 7 to day 42 were significant at $P < 0.001$. The collagen content in the skin of HOCl-injected mice and PBS-injected mice (broken horizontal line) is also shown (middle). The correlation between the collagen content in the skin and the skin thickness was determined in HOCl-injected mice ($r = 0.7486$, $P = 0.0013$ by Pearson's rank correlation test) (bottom). **B,** Expression of mRNA for *Col1*, *Col3*, *Tgfb1*, and *aSma* (normalized to *Tbp* expression) in the skin (left) and lungs (right) of HOCl-injected mice (expressed as the fold change compared with PBS-injected mice). Broken horizontal lines show the mean levels in PBS-injected mice. Values are the mean ± SEM of 8 mice per group. **C,** Representative sections of skin (original magnification × 10) and lung (original magnification × 20) obtained on day 42 from PBS- and HOCl-injected mice. Sections were stained with Masson's trichrome. **D,** Levels of advanced oxidation protein products (AOPPs) in sera from PBS- and HOCl-injected mice (expressed as chloramine T equivalents) (top). The total antioxidant capacity of sera from the 2 groups (expressed as Trolox equivalents) is also shown (middle). Serum levels of anti–Scl-70 antibody in the 2 groups were determined by enzyme-linked immunosorbent assay (optical density at 450 nm) (bottom). Each symbol represents a single mouse; horizontal lines with bars show the mean ± SEM. * = $P < 0.05$; ** = $P < 0.01$; *** = $P < 0.001$. Color figure can be viewed in the online issue, which is available at http://onlinelibrary.wiley.com/journal/doi/10.1002/art.39477/abstract.

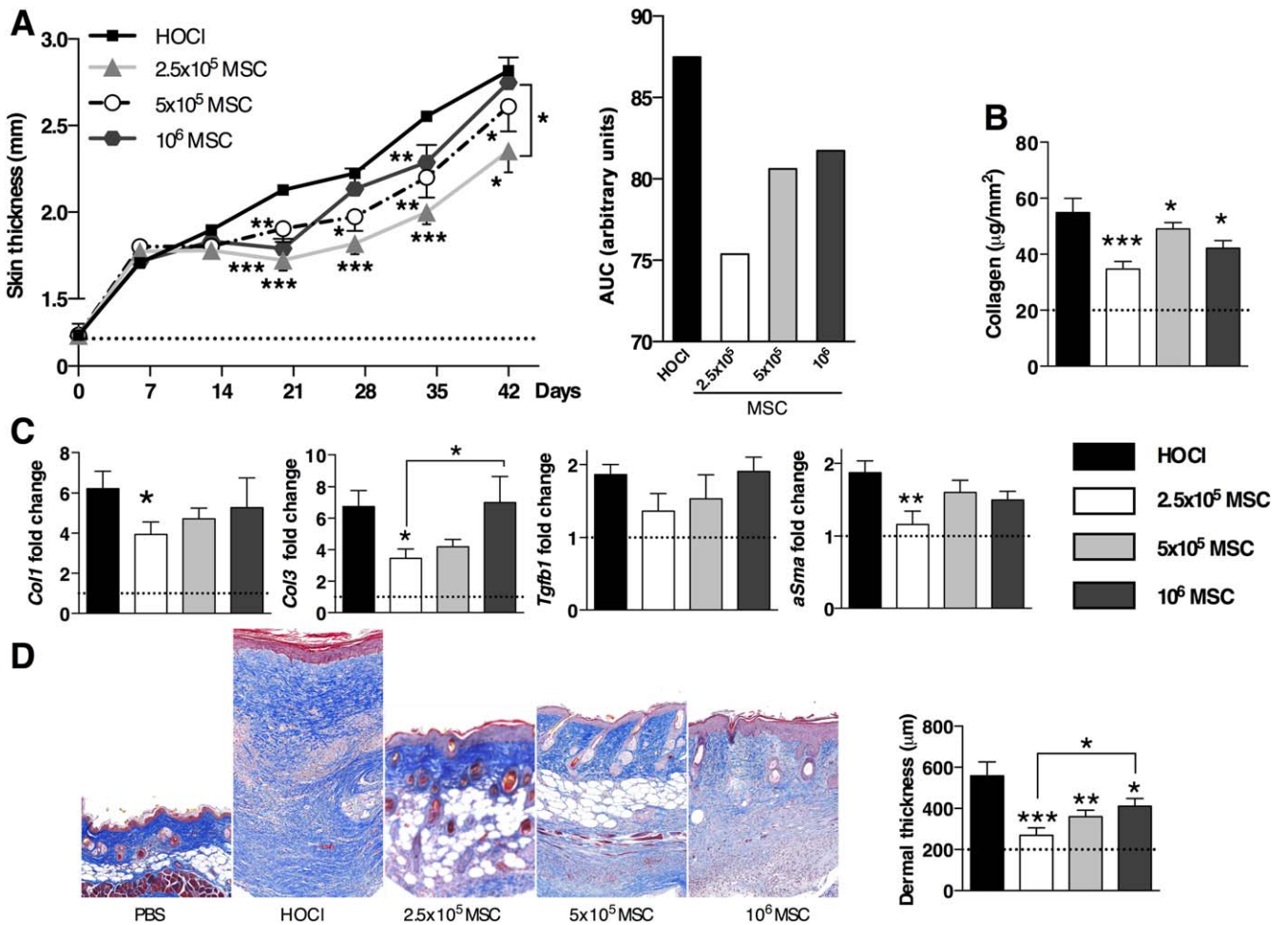

Figure 2. Reduced severity of skin fibrosis in HOCl-injected mice following a single infusion of 2.5×10^5 mesenchymal stem cells (MSCs). **A,** Skin thickness in HOCl-injected mice treated on day 0 with an infusion of 2.5×10^5, 5×10^5, or 10^6 MSCs as compared with untreated HOCl-injected (HOCl) mice. The area under the curve (AUC) for the evolution of skin thickening during the entire 6-week experiment in the HOCl-injected groups is shown at the right. **B,** Collagen content on day 42 in the skin of HOCl-injected mice treated with an infusion of MSCs at the indicated doses as compared with untreated HOCl-injected mice. **C,** Expression of mRNA for *Col1*, *Col3*, *Tgfb1*, *and aSma* (normalized to *Tbp* expression) on day 42 in skin samples from HOCl-injected mice treated with an infusion of MSCs at the indicated doses as compared with untreated HOCl-injected mice. Results are expressed as the fold change versus phosphate buffered saline (PBS)–injected mice. **D,** Representative skin sections obtained on day 42 from each of the experimental groups of mice. Sections were stained with Masson's trichrome. Original magnification × 10. The mean dermal thickness was measured in histologic sections of the skin, and the results are shown at the right. Broken horizontal lines show the mean levels in PBS-injected mice. Values are the mean ± SEM of 7–8 mice per group. $* = P < 0.05$; $** = P < 0.01$; $*** = P < 0.001$.

mice, HOCl-injected mice exhibited an early and progressive thickening of skin from day 7 to day 42 (Figure 1A). In HOCl-injected mice, progressive collagen deposition was noted in the skin and correlated with skin thickness, which could reliably predict fibrotic changes in skin (Figure 1A).

At the molecular level, mRNA for types I and III collagen exhibited peaks of expression on days 21 and 42 (Figure 1B). On day 42, the levels of *Col1* and *Col3* were, respectively, 10 and 7 times those observed in PBS-injected mice. Two other markers of fibrosis, *Tgfb1* and *aSma*, were statistically increased in HOCl-injected mice and expressed at similar levels from day 21 to day 42, except for day 28 (Figure 1B). Histologic analysis of fibrogenesis in the skin revealed a 2-step process. First, from day 14, we observed transparietal highly proliferative cellular infiltrates, which were even more obvious on day 21 (data available upon request from the corresponding author). This polymorphous infiltration included α-SMA+ and TGFβ+ myofibroblasts, as well as

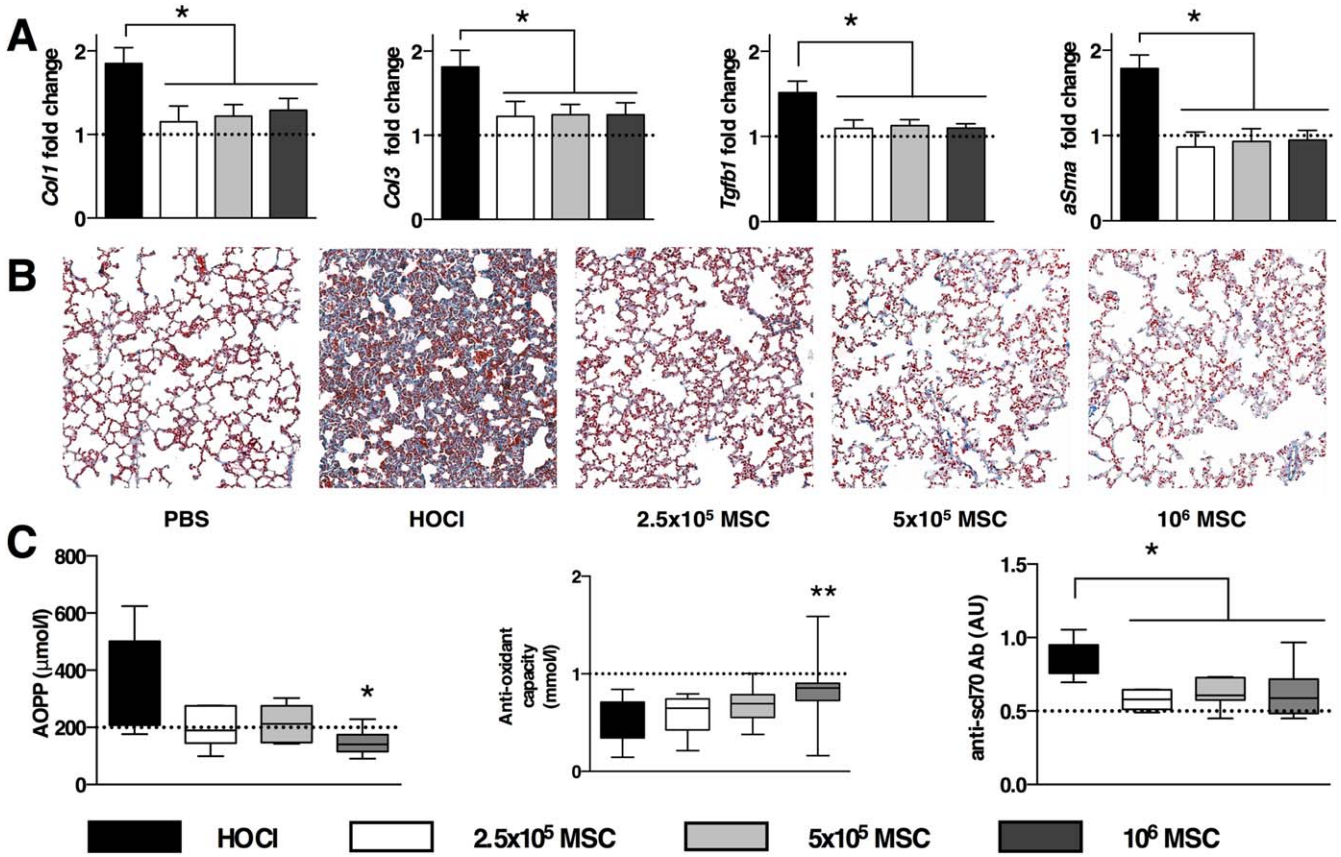

Figure 3. Prevention of the development of systemic symptoms in HOCl-injected mice by a single infusion of mesenchymal stem cells (MSCs) on day 0. **A,** Expression of mRNA for *Col1*, *Col3*, *Tgfb1*, and *aSma* (normalized to *Tbp* expression) on day 42 in lung samples from HOCl-injected mice treated on day 0 with different doses of MSCs as compared with untreated HOCl-injected (HOCl) mice. Results are expressed as the fold change compared with phosphate buffered saline (PBS)–injected mice. **B,** Representative lung sections obtained on day 42 from untreated PBS-injected, untreated HOCl-injected (HOCl), and HOCl-injected, MSC-treated (at the indicated doses) mice. Sections were stained with Masson's trichrome. Original magnification × 20. **C,** Levels of advanced oxidation protein products (AOPPs) in sera from untreated HOCl-injected and HOCl-injected, MSC-treated (at the indicated doses) mice (expressed as chloramine T equivalents) (left). The total antioxidant capacity of sera from these groups (expressed as Trolox equivalents) is also shown (middle). Serum levels of anti–Scl-70 antibody (Ab) in these groups were determined by enzyme-linked immunosorbent assay (optical density at 450 nm) (right). Broken horizontal lines show the mean levels in PBS-injected mice. Values are the mean ± SEM of 6–8 mice per group, except in **C**, where the data are shown as box plots. Each box represents the 25th to 75th percentiles. Lines inside the boxes represent the median. Lines outside the boxes represent the 10th and 90th percentiles. $* = P < 0.05$; $** = P < 0.01$. Color figure can be viewed in the online issue, which is available at http://onlinelibrary.wiley.com/journal/doi/10.1002/art.39477/abstract.

F4/80+ macrophages and CD3+ T lymphocytes (data available upon request from the corresponding author). We did not detect PAX-5+ B cells, however. In the second phase from day 21 to day 42, this cellular infiltration was progressively replaced by extracellular matrix (ECM) deposition, which disorganized all skin layers, resulting on day 42 in an intense thickening of the dermis and regression of hypodermic adipose tissue (Figure 1C and data not shown).

Fibrosis was also observed in the lungs, as indicated by the same markers as above. While *Col1* was only significantly increased on day 42, *Col3* expression was up-regulated as early as day 14 and significantly on days 14, 21, and 42 (Figure 1B). Similar profiles were noted for *Tgfb1* and *aSma* (Figure 1B). Histopathologic analysis corroborated these results, disclosing cell infiltration, thickening of pulmonary intraalveolar septa, and ECM deposition in HOCl-injected mice on day 42 (Figure 1C).

Finally, we confirmed the modulation of oxidative stress, as characterized by increased AOPP production and decreased total antioxidant capacity in sera from HOCl-injected mice (Figure 1D). In addition, the development of fibrosis was associated with the production of anti–Scl-70 autoantibodies (Figure 1D), as observed in human SSc and as has previously been des-

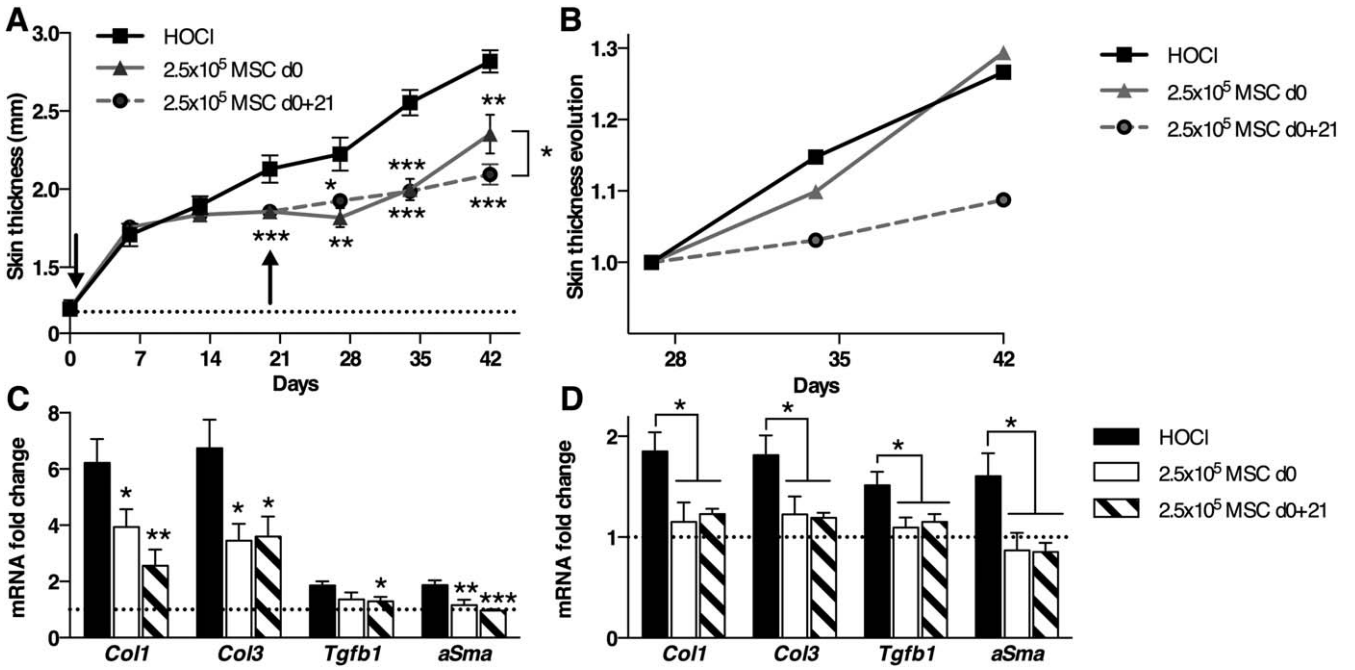

Figure 4. Improved effects of mesenchymal stem cells (MSCs) with a second infusion. **A,** Skin thickness in untreated HOCl-injected (HOCl) mice as compared with HOCl-injected mice treated with a single infusion of 2.5×10^5 MSCs on day 0 and with HOCl-injected mice given a second infusion of 2.5×10^5 MSCs on day 21. **Arrows** indicate MSC infusions. **B,** Fold change in skin thickness from day 28 to day 42 (normalized to day 28) in the same groups of mice as in **A**. **C** and **D,** Expression of mRNA for *Col1*, *Col3*, *Tgfb1*, and *aSma* (normalized to *Tbp* expression) on day 42 in skin samples (**C**) and in lung samples (**D**) from the 3 experimental groups. Results are expressed as the fold change compared with phosphate buffered saline (PBS)–injected mice. Broken horizontal lines show the mean levels in PBS-injected mice. Values are the mean ± SEM of 7–8 mice per group. $* = P < 0.05$; $** = P < 0.01$; $*** = P < 0.001$.

cribed in HOCl-injected mice (13). Taken together, these results confirmed that daily intradermal injections of HOCl in these mice induced diffuse SSc in a time-dependent manner.

Efficiency of a single infusion of MSCs for reducing both skin and lung fibrosis. The main objective of this study was to investigate the potential therapeutic role of MSCs in the HOCl model of SSc. We therefore evaluated the effect of a single systemic infusion of MSCs as a preventative by delivering a single infusion of 3 different doses of MSCs (2.5×10^5, 5×10^5, or 10^6) on day 0. We used bone marrow MSCs isolated from syngeneic mice, which were characterized by the expression of spinocerebellar ataxia type 1 (SCA-1), CD44, and CD73, and the absence of CD45 and CD11b. Cells were shown to differentiate into osteoblasts, adipocytes, and chondrocytes and to exert an immunosuppressive effect on the mitogen-induced proliferation of T lymphocytes (data available upon request from the corresponding author). Control groups (PBS-injected and untreated HOCl-injected mice) received an intravenous infusion of PBS.

Progression of skin fibrosis was similar in all groups until day 14 (Figure 2A). On day 21, the 3 MSC-treated groups exhibited 25–30% lower skin thickness as compared with the untreated HOCl-injected group (Figure 2A). However, the best results were obtained with the lowest dose of MSCs (2.5×10^5), with a sustained reduction of skin thickening throughout the experiment. At the end of the experiment (day 42), skin thickness was significantly lower in the group treated with 2.5×10^5 MSCs than in the group treated with 10^6 MSCs or in the untreated HOCl-injected group. This dose-related effect was also illustrated when measuring the area under the curve for the entire 6-week experiment (Figure 2A).

We then evaluated the effect of MSC infusion at the molecular and histologic level. The total collagen content in the skin on day 42 was significantly reduced in all MSC-treated groups, with the best results occurring with the lowest dose (Figure 2B). When considering the expression of transcripts for *Col1*, *Col3*, *Tgfb1*, and *aSma* in skin on day 42 (Figure 2C), a gradual dose-effect was observed that was inversely proportional to the MSC dose. Only the 2.5×10^5 dose of MSCs allowed a significant reduction in 3 of these 4 markers of fibrosis. Histologic analysis disclosed less ECM depo-

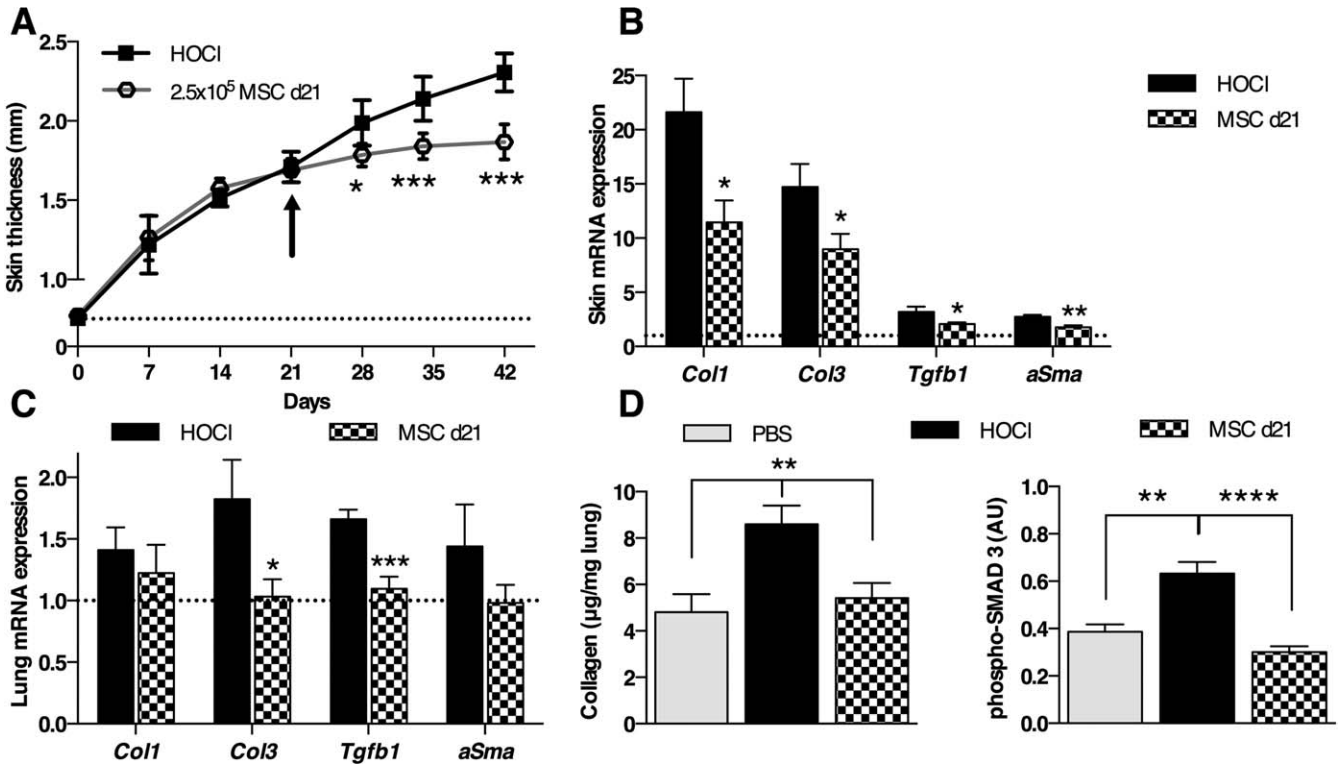

Figure 5. Improvement in skin and lung fibrosis with a single infusion of mesenchymal stem cells (MSCs) administered during the disease course. **A,** Skin thickness in HOCl-injected mice treated with 2.5×10^5 MSCs on day 21 (**arrow**) as compared with untreated HOCl-injected (HOCl) mice. **B** and **C,** Expression of mRNA for *Col1*, *Col3*, *Tgfb1*, and *aSma* (normalized to *Tbp* expression) on day 42 in skin samples (**B**) and in lung samples (**C**) from the 2 experimental groups. Results are expressed as the fold change compared with phosphate buffered saline (PBS)–injected mice. Broken horizontal lines show the mean levels in PBS-injected mice. **D,** Collagen content (left) and phosphorylated Smad3 levels (right) in lung samples obtained on day 42 from PBS-injected mice, untreated HOCl-injected mice, and HOCl-injected, MSC-treated mice. Values are the mean ± SEM of at least 8 mice per group in **A**, **B**, and **D**, and 7–8 mice per group in **C**. $* = P < 0.05$; $** = P < 0.01$; $*** = P < 0.001$.

sition and cellular infiltration in the MSC-treated mice, which was related to the dose and was also evidenced by dermal thickness (Figure 2D).

The expression of mRNA for the fibrosis markers *Col1*, *Col3*, *Tgfb1*, and *aSma* in lung tissues was decreased by the same proportion in the 3 MSC-treated groups and reached the levels in healthy mice (Figure 3A). Histologic analysis revealed fewer fibrotic lesions in the MSC-treated groups than in the untreated HOCl-injected group, whatever the dose of MSCs infused (Figure 3B). More precisely, intraalveolar septa exhibited almost normal architecture in the MSC-treated groups, with fewer parenchymal cell infiltrates.

With regard to the parameters of systemic oxidation, decreased serum AOPP production (Figure 3C) was observed in all MSC-treated groups, significantly so in the 10^6 MSC-treated group. The highest dose was also associated with higher serum antioxidant capacity, reaching the levels in the untreated PBS-injected mice (Figure 3C). In parallel, serum levels of anti–Scl-70 antibody were significantly reduced whatever the dose infused (Figure 3C). In summary, MSC infusion before disease induction reduced all parameters of fibrosis in both skin and lung in these mice. Notably, the most efficient therapeutic effect was observed with the lowest dose of 2.5×10^5 MSCs.

Improvement in the therapeutic effects of a second infusion of MSCs. Although skin thickness was improved in MSC-treated, HOCl-injected mice, the disease progression in this group paralleled that in the untreated HOCl-injected mice after day 21 (slope = 0.0197 and 0.01768 mm/day, respectively, from day 28 to day 42) (Figure 2A), and no additional benefit was observed after this time point. We therefore hypothesized that a second infusion of MSCs on day 21 might allow sustained slowing of disease progression. When compared to the group treated on day 0, the group receiving MSCs on day 0 and day 21 showed a slower progression of skin thickening from day 28 to day 42,

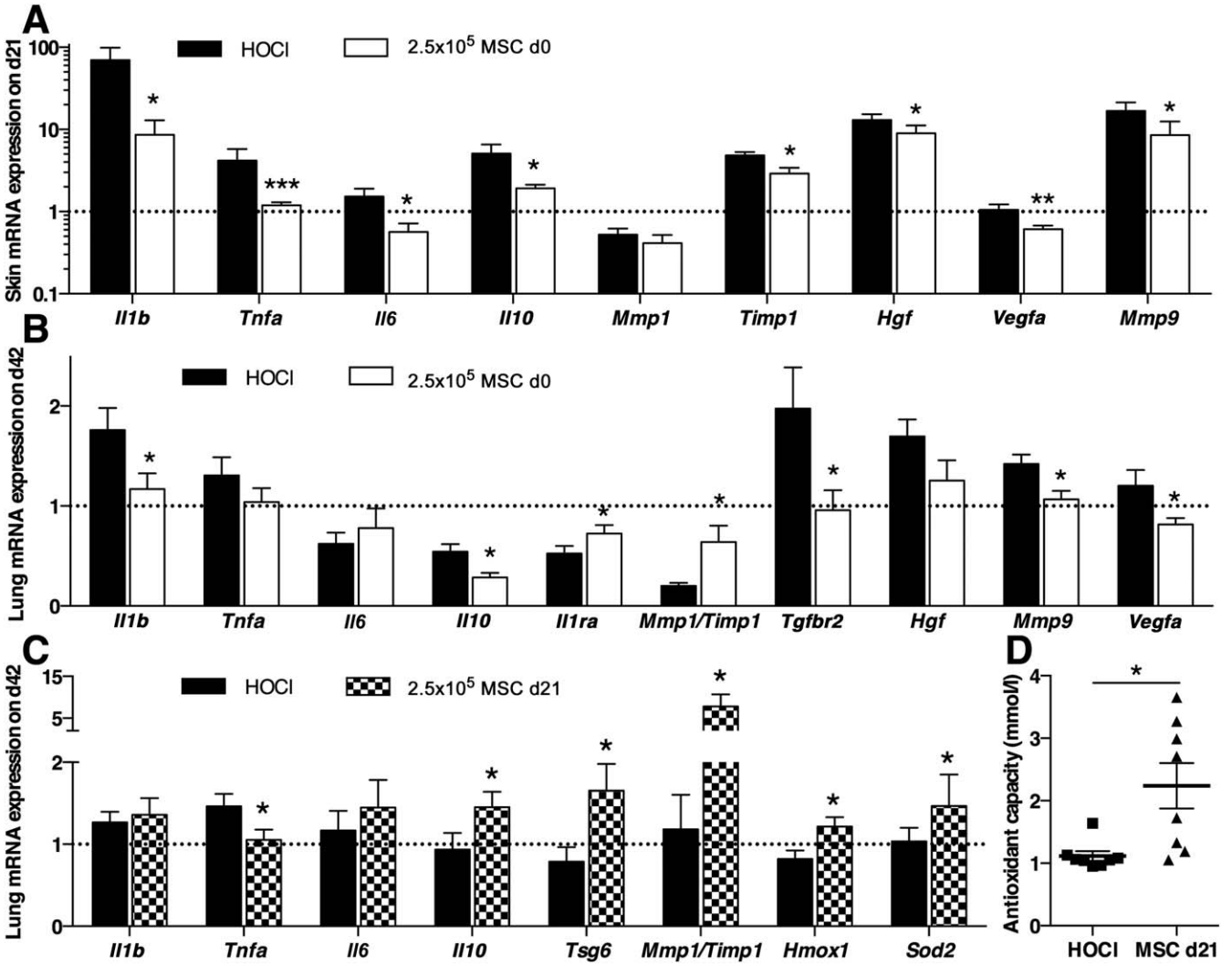

Figure 6. Association of reduced fibrosis in HOCl-injected mice treated with mesenchymal stem cells (MSCs) with changes in extracellular matrix remodeling and in parameters of inflammation and oxidation. **A** and **B,** Expression of mRNA for the indicated genes (normalized to *Tbp* expression) on day 21 in skin samples (**A**) and on day 42 in lung samples (**B**) from untreated HOCl-injected (HOCl) mice as compared with HOCl-injected mice treated on day 0 with MSCs. Results are expressed as the fold change as compared with phosphate buffered saline (PBS)–injected mice. **C,** Expression of mRNA for the indicated genes on day 42 in lung samples from untreated HOCl-injected mice as compared with HOCl-injected mice treated on day 21 with MSCs (normalized to *Tbp* expression). Broken horizontal lines show the mean levels in PBS-injected mice. Values are the mean ± SEM of 8 mice per group. **D,** Total antioxidant capacity of sera from untreated HOCl-injected mice as compared with HOCl-injected mice treated on day 21 with MSCs (expressed as Trolox equivalents). Each symbol represents a single mouse; horizontal lines with bars show the mean ± SEM. $* = P < 0.05$; $** = P < 0.01$; $*** = P < 0.001$.

resulting in an additional 15% improvement on day 42 (slope = 0.0197 and 0.005869, respectively, from day 28 to day 42) (Figures 4A and B). Accordingly, a stronger decrease in the expression of the fibrosis markers *Col1*, *Tgfb1*, and *aSma* in skin was noted in this group treated on day 0 plus day 21 (Figure 4C). However, no further improvement was noted in the lungs, since the levels of these markers of fibrosis were already normalized by a single infusion of MSCs (Figure 4D).

Improvement in both skin and lung fibrosis after a single infusion of MSCs during the disease course. We next investigated whether MSCs might exert beneficial effects on skin and lung fibrosis after the SSc had become established. We therefore studied the effect of a late single infusion of MSCs on day 21 in a curative approach. Interestingly, a single infusion on day 21 blocked disease progression 1 week after treatment and continued until the end of the experiment (Figure 5A).

Moreover, the day 21 infusion resulted in a significant reduction in the expression of *Col1*, *Col3*, *Tgfb1*, and *aSma* in the skin (Figure 5B) and a significant reduction of *Col3* and *Tgfb1* in the lung (Figure 5C). These results were corroborated by the finding of less deposition of collagen in lung tissue as compared with that in untreated HOCl-injected mice (Figure 5D), as well as a lower level of Smad3 phosphorylation (Figure 5D). Most notably, both parameters reached the levels found in healthy mice. These results therefore indicate that a single infusion of 2.5×10^5 MSCs is effective as a curative approach in these mice after the SSc phenotype has become established.

Association between the therapeutic effect of MSCs in HOCl-injected mice and changes in tissue remodeling and inflammatory and oxidative parameters. In order to better understand the antifibrotic effects of MSCs observed in the lung and skin samples, we investigated the molecular mechanisms that might be involved. We first focused on mice euthanized on day 21, since day 21 was a crucial time point for the development of fibrosis in HOCl-injected mice (Figures 1A and B) and was also the time point at which MSCs injected on day 0 had the most important effect on skin thickness reduction (Figure 2A).

On day 21, MSC-treated mice exhibited lower levels of mRNA for the cytokines *Il1b*, *Tnfa*, *Il6*, and *Il10* in the skin as compared with the expression in untreated HOCl-injected mice (Figure 6A). Histologic analysis disclosed fewer Ki-67+ proliferative cellular infiltrates and fewer CD3+ and F4/80+ cells (data available upon request from the corresponding author). Interestingly, MSC treatment also led to a reduced expression of transcripts for tissue remodeling parameters, such as *Timp1*, *Hgf*, *Vegfa*, and *Mmp9*, in the skin on day 21 (Figure 6A). However, on day 42, only *Tnfa* and *Il6* were significantly lower in the MSC-treated group, suggesting a time-limited effect of MSCs (data available upon request from the corresponding author). Of note, a second infusion of MSCs on day 21 led to a normalization or decrease in the expression of mRNA for all of the above-mentioned genes, indicating a better therapeutic effect (data available upon request from the corresponding author). Anti-inflammatory and remodeling effects were also observed on day 42 in mice treated with a single infusion of MSCs on day 21 (data available upon request from the corresponding author).

We then focused on the lung tissues examined on day 42 and observed a down-regulation of *Il1b*, *Tnfa*, and *Il10* in mice treated with MSCs on day 0, as well as an up-regulation of *Il1ra* (Figure 6B). Tissue remodeling parameters were also affected by MSC treatment, as illustrated by a significant up-regulation of the *Mmp1*:*Timp1* ratio, together with a down-regulation of *Tgfbr2*, *Hgf*, *Mmp9*, and *Vegfa* expression (Figure 6B). Interestingly, MSC infusion on day 21 resulted in a different cytokine response in the lung. This was characterized by a lower expression of *Tnfa*, together with an up-regulation of *Il10* and *Tsg6* (Figure 6C). Of note, this curative approach also led to a significant increase in the *Mmp1*:*Timp1* ratio (Figure 6C).

We also searched for possible antioxidant mechanisms in day 21–treated mice and noted a significant up-regulation of the expression of mRNA for the antioxidant enzymes *Hmox1* and *Sod2* in the lung (Figure 6C) and for *Sod2* in the skin (data not shown). These findings could be related to an enhanced antioxidant capacity of serum in these mice (Figure 6D).

Taken together, all of these results indicate that MSCs counteract the effects of oxidation-induced damage and fibrotic processes in HOCl-injected mice. These effects are mainly mediated through the tissue modulation of ECM remodeling, inflammation, and antioxidant machinery.

DISCUSSION

This study provides original preclinical data concerning MSCs as a potent treatment in a relevant murine model of the diffuse form of SSc. We demonstrated that administration of MSCs is efficient in reducing inflammatory, oxidative, and fibrotic processes. Importantly, MSCs had the ability to not only counteract SSc induction when injected preventively, but also reduce the severity of systemic involvement in a curative approach once the disease was established.

Prior to the present study, the therapeutic properties of MSCs had only been described in the rodent acute lung injury model, in which infusions of MSCs were given during the first hours or days following intratracheal instillation of bleomycin (17–22). Those studies gave evidence of the ability of systemically infused MSCs to home to the injured regions of the lungs, where they exerted an antiinflammatory effect (11). However, none of the previously reported studies examined either chronic lung fibrosis after repeated bleomycin intratracheal instillations or systemic fibrosis after repeated intradermal bleomycin injections, and thus, the studies did not consider all of the features of SSc. Moreover, in the systemic bleomycin model, there was no mention of AOPPs or specific anti–Scl-70 antibodies (12). It was for these reasons that we chose the HOCl-induced mouse model of SSc described by Servettaz et al (13) since it is analogous to diffuse SSc in humans.

We have now added to the initially reported information our own findings concerning the analysis of fibrosis development at the molecular level and the time dependency of the changes. We demonstrated that types I and III collagen were highly induced, and we confirmed the pivotal role of TGFβ pathway activation in the process. We also noted the overexpression of TGFβ receptor type II in tissues, as has been described in human SSc (23,24) and in a genetic mouse model of the disease (25).

In our study, MSCs showed a protective effect on skin fibrosis, which was inversely proportional to the MSC dose, with the best results on all molecular markers occurring with the lowest dose of MSCs examined (2.5×10^5). Interestingly, these dose-related effects affected only the skin, as most of the markers in the lung were decreased to the levels in healthy mice with each of the 3 MSC doses we examined. MSCs prevented the onset of lung fibrosis in treated mice, as documented by the normal parenchymal architecture in the absence of fibrotic lesions and inflammatory infiltrates. These substantial effects likely resulted from the abundance of MSCs in the lung, since it is the primary target of systemically infused MSCs.

One explanation for the inverse dose effect of MSCs in the skin might be that a greater number were trapped in the lung following the occurrence of microemboli. We believe this was not the case, since we did not detect any recruitment of the cells to the skin at the sensitivity limit of the technique we used (data available upon request from the corresponding author). Although we cannot fully explain the inversely proportional effects of the MSC dose on the skin, the effects are consistent with those reported in other studies (26–28). Nevertheless, few dose-escalation studies have been reported, and positive dose-related effects were usually observed (29,30). These contradictory results are likely due to the source of the stem cells, the pathologic environment, and the timing and route of injection. Another possible explanation for the inverse dose effect may be connected to the release of cytokines by MSCs that can determine contrasting biologic responses at low and high concentrations. Taken together, it seems that "more is not always better and the minimum and maximum effective doses must be determined based on the clinical application," as asserted by Murphy et al (28).

In our preventive approach, MSCs seemed to have a time-limited effect, characterized by a maximum impact on skin on day 21, followed by a progressive escape. One possible reason for this may be related to the survival of MSCs in the tissues. Indeed, despite their ability to migrate to injured tissues, MSCs are rapidly cleared after systemic infusion (20,31), yet the benefits can be observed long after their disappearance and support a "hit and run" mechanism rather than a long-term engraftment in tissues (32). Consistent with this, benefits were observed in our study while MSCs did not migrate to the skin and did not persist in the lungs for more than a couple of days (data available upon request from the corresponding author). The long-lasting effects of MSCs have thus been proposed to stem from paracrine secretion of soluble factors or microvesicles, such as exosomes (33). A second reason for this time-limited effect may be directly due to the SSc model we used. Indeed, continuous injections of HOCl during the entire experiment undoubtedly contributed to disease progression and, thus, to a limitation of MSC benefits. These two ideas are also supported by the benefits obtained with the late injection on day 21. These benefits are particularly valuable considering that fibrosis was already established at this time.

In our model, the therapeutic effects of MSCs likely involve their ability to secrete antiinflammatory cytokines and trophic molecules, even if their ability to differentiate into alveolar epithelial cells could account for their regenerative potential (17,20). The antiinflammatory effects of MSCs are well documented and primarily depend on paracrine mechanisms (34,35). Similar to previous studies in rodent models of lung diseases, we found an up-regulation of *Il1ra* and *Tsg6* in the lungs of treated mice, combined with a steady down-regulation of inflammatory cytokines (11,19,36). We also noted lower levels of autoantibodies in MSC-treated mice, suggesting reduced B cell activation. Interestingly, we showed that IL-10 secretion in lung depended on the timing of MSC infusion, resulting in an early up-regulation of the gene expression, followed by a strong down-regulation. Indeed, the role of this cytokine in fibrotic processes remains a topic of controversy (37–39). Most commonly recognized as an antiinflammatory cytokine in acute lung injury, long-term overexpression of *Il10* has also been associated with the development of fibrosis (40,41).

This study is the first to show the dysregulation of tissue remodeling activity in the HOCl model, consistent with available data on human SSc and the efficacy of MSCs in reverting this pathologic process (42). First, MSC infusion augmented the *Mmp1:Timp1* ratio, promoting clearance of fibrosis in tissues. Second, MSC infusion down-regulated other metalloproteinases whose biologic properties differ from those of *Mmp1* (i.e., *Mmp9* and *Mmp2* [data not shown]). These other MMPs are known as gelatinases, and they exhibit no collagenase activity. These 2 enzymes may contribute to

tissue inflammation through neoangiogenesis and recruitment of neutrophils (43). Third, MSCs were able to normalize the increased expression of vascular remodeling factors in the skin of HOCl-injected mice, such as *Pecam1* (data not shown) and *Vegfa*, the latter currently under discussion as a new therapeutic target in SSc (44,45). Finally, MSCs partially reverted the strong increase in *Hgf* observed in the skin of HOCl-injected mice. Although *Hgf* has pleiotropic actions and may have an antifibrotic effect, it is also increased in human SSc and is associated with disease severity (42).

We also demonstrated that MSCs exert their therapeutic effects by increasing the antioxidant defenses of animals. Indeed, MSC infusion was associated with an up-regulation of antioxidant enzymes in target tissues, leading to an increased total antioxidant capacity and reduced levels of AOPPs in mouse sera. This is of particular interest considering the high levels of AOPPs in SSc and their potential to dysregulate fibroblast and endothelial cell proliferation in vitro (16). AOPPs are considered not only markers of oxidative stress in SSc, but also vectors of systemic fibrosis, vasculopathy, and breach of self tolerance (13). In this regard, the antioxidant effect of MSCs as described in other diseases seems appealing (46–48). On the whole, the pleiotropic effects we observed, which lasted long after MSC survival in the tissues, could result from crosstalk between healthy infused MSCs and the environment, including resident progenitor cells. Several recent studies have shown that abnormal stem cell activation might drive fibrogenesis in animal models (49,50) as well as in human SSc (24). A possible explanation might be that the reintroduction of exogenous healthy MSCs could revert the altered phenotype of resident progenitor cells and restore their ability to counteract the pathologic process.

In conclusion, we demonstrate the therapeutic effects of systemic infusion of MSCs in a relevant model of diffuse SSc, both in a preventive as well as in a curative approach after disease clinical onset. Taken together, our results support the pleiotropic effects of MSCs following activation by the surrounding oxidative environment and acting through antiinflammatory and antioxidative responses, as well as tissue remodeling. These promising results obtained in murine SSc hold new hope for upcoming clinical trials of MSCs in this multifaceted disease.

ACKNOWLEDGMENTS

We thank the Réseau des Animaleries de Montpellier animal facility, the Montpellier RIO Imaging platform, and the Réseau d'Histologie Expérimentale de Montpellier histology facility, in particular Yoan Buscail, for processing the animal tissues used in our study. We also thank Sylvie Modurier for proofreading the manuscript.

AUTHOR CONTRIBUTIONS

All authors were involved in drafting the article or revising it critically for important intellectual content, and all authors approved the final version to be published. Dr. Noël had full access to all of the data in the study and takes responsibility for the integrity of the data and the accuracy of the data analysis.

Study conception and design. Maria, Le Quellec, Jorgensen, Noël, Guilpain.

Acquisition of data. Maria, Toupet, Bony, Pirot, Vozenin, Petit, Roger, Noël, Guilpain.

Analysis and interpretation of data. Maria, Pirot, Vozenin, Batteux, Le Quellec, Jorgensen, Noël, Guilpain.

REFERENCES

1. Walker KM, Pope J, participating members of the Scleroderma Clinical Trials Consortium (SCTC), Canadian Scleroderma Research Group (CSRG). Treatment of systemic sclerosis complications: what to use when first-line treatment fails—a consensus of systemic sclerosis experts. Semin Arthritis Rheum 2012;42:42–55.
2. Van Laar JM, Sullivan K. Stem cell transplantation in systemic sclerosis. Curr Opin Rheumatol 2013;25:719–25.
3. Cipriani P, Carubbi F, Liakouli V, Marrelli A, Perricone C, Perricone R, et al. Stem cells in autoimmune diseases: implications for pathogenesis and future trends in therapy. Autoimmun Rev 2013;12:709–16.
4. Maumus M, Guerit D, Toupet K, Jorgensen C, Noel D. Mesenchymal stem cell-based therapies in regenerative medicine: applications in rheumatology. Stem Cell Res Ther 2011;2:14.
5. Zhou H, Guo M, Bian C, Sun Z, Yang Z, Zeng Y, et al. Efficacy of bone marrow-derived mesenchymal stem cells in the treatment of sclerodermatous chronic graft-versus-host disease: clinical report. Biol Blood Marrow Transplant 2010;16:403–12.
6. Connick P, Kolappan M, Crawley C, Webber DJ, Patani R, Michell AW, et al. Autologous mesenchymal stem cells for the treatment of secondary progressive multiple sclerosis: an open-label phase 2a proof-of-concept study. Lancet Neurol 2012;11:150–6.
7. Wang D, Li J, Zhang Y, Zhang M, Chen J, Li X, et al. Umbilical cord mesenchymal stem cell transplantation in active and refractory systemic lupus erythematosus: a multicenter clinical study. Arthritis Res Ther 2014;16:R79.
8. De la Portilla F, Alba F, Garcia-Olmo D, Herrerias JM, Gonzalez FX, Galindo A. Expanded allogeneic adipose-derived stem cells (eASCs) for the treatment of complex perianal fistula in Crohn's disease: results from a multicenter phase I/IIa clinical trial. Int J Colorectal Dis 2013;28:313–23.
9. Guiducci S, Porta F, Saccardi R, Guidi S, Ibba-Manneschi L, Manetti M, et al. Autologous mesenchymal stem cells foster revascularization of ischemic limbs in systemic sclerosis: a case report. Ann Intern Med 2010;153:650–4.
10. Keyszer G, Christopeit M, Fick S, Schendel M, Taute BM, Behre G, et al. Treatment of severe progressive systemic sclerosis with transplantation of mesenchymal stromal cells from allogeneic related donors: report of five cases. Arthritis Rheum 2011;63:2540–2.
11. Inamdar AC, Inamdar AA. Mesenchymal stem cell therapy in lung disorders: pathogenesis of lung diseases and mechanism of action of mesenchymal stem cell. Exp Lung Res 2013;39:315–27.

12. Batteux F, Kavian N, Servettaz A. New insights on chemically induced animal models of systemic sclerosis. Curr Opin Rheumatol 2011;23:511–8.
13. Servettaz A, Goulvestre C, Kavian N, Nicco C, Guilpain P, Chereau C, et al. Selective oxidation of DNA topoisomerase 1 induces systemic sclerosis in the mouse. J Immunol 2009;182: 5855–64.
14. Bouffi C, Bony C, Courties G, Jorgensen C, Noel D. IL-6-dependent PGE2 secretion by mesenchymal stem cells inhibits local inflammation in experimental arthritis. PloS One 2010;5: e14247.
15. Toupet K, Maumus M, Peyrafitte JA, Bourin P, van Lent PL, Ferreira R, et al. Long-term detection of human adipose-derived mesenchymal stem cells after intraarticular injection in SCID mice. Arthritis Rheum 2013;65:1786–94.
16. Servettaz A, Guilpain P, Goulvestre C, Chereau C, Hercend C, Nicco C, et al. Radical oxygen species production induced by advanced oxidation protein products predicts clinical evolution and response to treatment in systemic sclerosis. Ann Rheum Dis 2007;66:1202–9.
17. Ortiz LA, Gambelli F, McBride C, Gaupp D, Baddoo M, Kaminski N, et al. Mesenchymal stem cell engraftment in lung is enhanced in response to bleomycin exposure and ameliorates its fibrotic effects. Proc Natl Acad Sci U S A 2003;100:8407–11.
18. Rojas M, Xu J, Woods CR, Mora AL, Spears W, Roman J, et al. Bone marrow-derived mesenchymal stem cells in repair of the injured lung. Am J Respir Cell Mol Biol 2005;33:145–52.
19. Ortiz LA, Dutreil M, Fattman C, Pandey AC, Torres G, Go K, et al. Interleukin 1 receptor antagonist mediates the antiinflammatory and antifibrotic effect of mesenchymal stem cells during lung injury. Proc Natl Acad Sci U S A 2007;104:11002–7.
20. Zhao F, Zhang YF, Liu YG, Zhou JJ, Li ZK, Wu CG, et al. Therapeutic effects of bone marrow-derived mesenchymal stem cells engraftment on bleomycin-induced lung injury in rats. Transplant Proc 2008;40:1700–5.
21. Cargnoni A, Gibelli L, Tosini A, Signoroni PB, Nassuato C, Arienti D, et al. Transplantation of allogeneic and xenogeneic placenta-derived cells reduces bleomycin-induced lung fibrosis. Cell Transplant 2009;18:405–22.
22. Moodley Y, Atienza D, Manuelpillai U, Samuel CS, Tchongue J, Ilancheran S, et al. Human umbilical cord mesenchymal stem cells reduce fibrosis of bleomycin-induced lung injury. Am J Pathol 2009;175:303–13.
23. Kubo M, Ihn H, Yamane K, Tamaki K. Up-regulated expression of transforming growth factor β receptors in dermal fibroblasts in skin sections from patients with localized scleroderma. Arthritis Rheum 2001;44:731–4.
24. Vanneaux V, Farge-Bancel D, Lecourt S, Baraut J, Cras A, Jean-Louis F, et al. Expression of transforming growth factor β receptor II in mesenchymal stem cells from systemic sclerosis patients. BMJ Open 2013;3:e001890.
25. Denton CP, Zheng B, Evans LA, Shi-wen X, Ong VH, Fisher I, et al. Fibroblast-specific expression of a kinase-deficient type II transforming growth factor β (TGFβ) receptor leads to paradoxical activation of TGFβ signaling pathways with fibrosis in transgenic mice. J Biol Chemistry 2003;278:25109–19.
26. Hashemi SM, Ghods S, Kolodgie FD, Parcham-Azad K, Keane M, Hamamdzic D, et al. A placebo controlled, dose-ranging, safety study of allogenic mesenchymal stem cells injected by endomyocardial delivery after an acute myocardial infarction. Eur Heart J 2008;29:251–9.
27. Desando G, Cavallo C, Sartoni F, Martini L, Parrilli A, Veronesi F, et al. Intra-articular delivery of adipose derived stromal cells attenuates osteoarthritis progression in an experimental rabbit model. Arthritis Res Ther 2013;15:R22.
28. Murphy MB, Moncivais K, Caplan AI. Mesenchymal stem cells: environmentally responsive therapeutics for regenerative medicine. Exp Mol Med 2013;45:e54.
29. Wolf D, Reinhard A, Seckinger A, Katus HA, Kuecherer H, Hansen A. Dose-dependent effects of intravenous allogeneic mesenchymal stem cells in the infarcted porcine heart. Stem Cells Dev 2009;18:321–9.
30. Joo SY, Cho KA, Jung YJ, Kim HS, Park SY, Choi YB, et al. Mesenchymal stromal cells inhibit graft-versus-host disease of mice in a dose-dependent manner. Cytotherapy 2010;12:361–70.
31. Von Bahr L, Batsis I, Moll G, Hagg M, Szakos A, Sundberg B, et al. Analysis of tissues following mesenchymal stromal cell therapy in humans indicates limited long-term engraftment and no ectopic tissue formation. Stem Cells 2012;30:1575–8.
32. Ankrum JA, Ong JF, Karp JM. Mesenchymal stem cells: immune evasive, not immune privileged. Nat Biotechnol 2014;32: 252–60.
33. Maumus M, Jorgensen C, Noel D. Mesenchymal stem cells in regenerative medicine applied to rheumatic diseases: role of secretome and exosomes. Biochimie 2013;95:2229–34.
34. Djouad F, Bouffi C, Ghannam S, Noel D, Jorgensen C. Mesenchymal stem cells: innovative therapeutic tools for rheumatic diseases. Nat Rev Rheumatol 2009;5:392–9.
35. Conese M, Carbone A, Castellani S, Di Gioia S. Paracrine effects and heterogeneity of marrow-derived stem/progenitor cells: relevance for the treatment of respiratory diseases. Cells Tissues Organs 2013;197:445–73.
36. Lee RH, Pulin AA, Seo MJ, Kota DJ, Ylostalo J, Larson BL, et al. Intravenous hMSCs improve myocardial infarction in mice because cells embolized in lung are activated to secrete the anti-inflammatory protein TSG-6. Cell Stem Cell 2009;5:54–63.
37. Garantziotis S, Brass DM, Savov J, Hollingsworth JW, McElvania-TeKippe E, Berman K, et al. Leukocyte-derived IL-10 reduces subepithelial fibrosis associated with chronically inhaled endotoxin. Am J Respir Cell Mol Biol 2006;35:662–7.
38. Nakagome K, Dohi M, Okunishi K, Tanaka R, Miyazaki J, Yamamoto K. In vivo IL-10 gene delivery attenuates bleomycin induced pulmonary fibrosis by inhibiting the production and activation of TGF-β in the lung. Thorax 2006;61:886–94.
39. Lee CG, Homer RJ, Cohn L, Link H, Jung S, Craft JE, et al. Transgenic overexpression of interleukin (IL)$-$10 in the lung causes mucus metaplasia, tissue inflammation, and airway remodeling via IL-13-dependent and -independent pathways. J Biol Chem 2002;277:35466–74.
40. Spight D, Zhao B, Haas M, Wert S, Denenberg A, Shanley TP. Immunoregulatory effects of regulated, lung-targeted expression of IL-10 in vivo. Am J Physiol Lung Cell Mol Physiol 2005;288: L251–65.
41. Sun L, Louie MC, Vannella KM, Wilke CA, LeVine AM, Moore BB, et al. New concepts of IL-10-induced lung fibrosis: fibrocyte recruitment and M2 activation in a CCL2/CCR2 axis. Am J Physiol Lung Cell Mol Physiol 2011;300:L341–53.
42. Frost J, Ramsay M, Mia R, Moosa L, Musenge E, Tikly M. Differential gene expression of MMP-1, TIMP-1 and HGF in clinically involved and uninvolved skin in South Africans with SSc. Rheumatology (Oxford) 2012;51:1049–52.
43. Khokha R, Murthy A, Weiss A. Metalloproteinases and their natural inhibitors in inflammation and immunity. Nat Rev Immunol 2013;13:649–65.
44. Cipriani P, Di Benedetto P, Capece D, Zazzeroni F, Liakouli V, Ruscitti P, et al. Impaired Cav-1 expression in SSc mesenchymal cells upregulates VEGF signaling: a link between vascular involvement and fibrosis. Fibrogenesis Tissue Repair 2014;7:13.
45. Kavian N, Servettaz A, Marut W, Nicco C, Chereau C, Weill B, et al. Sunitinib inhibits the phosphorylation of platelet-derived growth factor receptor β in the skin of mice with scleroderma-like features and prevents the development of the disease. Arthritis Rheum 2012;64:1990–2000.
46. Islam MN, Das SR, Emin MT, Wei M, Sun L, Westphalen K, et al. Mitochondrial transfer from bone-marrow-derived stromal cells to pulmonary alveoli protects against acute lung injury. Nat Med 2012;18:759–65.

47. Lee C, Mitsialis SA, Aslam M, Vitali SH, Vergadi E, Konstantinou G, et al. Exosomes mediate the cytoprotective action of mesenchymal stromal cells on hypoxia-induced pulmonary hypertension. Circulation 2012;126:2601–11.
48. Cho KA, Woo SY, Seoh JY, Han HS, Ryu KH. Mesenchymal stem cells restore CCl4-induced liver injury by an antioxidative process. Cell Biol Int 2012;36:1267–74.
49. Marangoni RG, Korman BD, Wei J, Wood TA, Graham LV, Whitfield ML, et al. Myofibroblasts in murine cutaneous fibrosis originate from adiponectin-positive intradermal progenitors. Arthritis Rheumatol 2015;67:1062–73.
50. Liu S, Herault Y, Pavlovic G, Leask A. Skin progenitor cells contribute to bleomycin-induced skin fibrosis. Arthritis Rheumatol 2014;66:707–13.

DOI 10.1002/art.39688

Erratum

In the editorial by Sattar and McInnes published in the March 2016 issue of *Arthritis & Rheumatology* (pages 563–565), financial disclosure information had been provided to the journal by Dr. Sattar but was inadvertently not included in the published piece. The information is as follows: "Dr. Sattar has received consulting fees, speaking fees, and/or honoraria from Merck, Amgen, and Sanofi (less than $10,000 each)."

We regret the errors.